JOURNAL OF PROPULSION AND POWER
Vol. 27, No. 2, March–April 2011

Updated Kinetic Mechanism for High-Pressure Hydrogen Combustion

Kazuya Shimizu,* Atsushi Hibi,† and Mituso Koshi‡
University of Tokyo, Tokyo 113-8656, Japan
Youhi Morii§
Graduate University for Advanced Studies, Kanagawa 229-8510, Japan
and
Nobuyuki Tsuboi¶
Kyusyu Institute of Technology, Kitakyusyu 804-8550, Japan

DOI: 10.2514/1.48553

A chemical kinetic model for high-pressure combustion of H_2/O_2 mixtures has been developed by updating some of the rate constants important under high-pressure conditions without any diluent. The revised mechanism is validated against experimental shock-tube ignition delay times and laminar flame speeds. Predictions of the present model are also compared with those by several other kinetic models proposed recently. Although predictions of those models (including the present model) agree quite well with each other and with the experimental data of ignition delay times and flame speeds at pressures lower than 10 atm, substantial differences are observed between recent experimental data of high-pressure mass burning rates and model predictions, as well as among the model predictions themselves. Different pressure dependencies of mass burning rates above 10 atm in different kinetic models result from using different rate constants in these models for HO_2 reactions, especially for $H + HO_2$ and $OH + HO_2$ reactions. The rate constants for the reaction $H + HO_2$ involving different product channels were found to be very important for the prediction of high-pressure combustion characteristics. An updated choice of rate constants for those reactions is presented on the basis of recent experimental and theoretical studies. The role of $O(^1D)$, which can be produced by the $H + HO_2$ reaction, in the high-pressure combustion of H_2 is discussed.

Nomenclature

A	=	preexponential factor
E_a	=	activation energy
F_c	=	Troe parameter
k	=	rate constant
k_0	=	low-pressure limiting rate constant
M	=	third body
n	=	temperature exponent
p	=	pressure
R	=	universal gas constant
S_u	=	laminar flame speed
T	=	temperature
ρ	=	density
τ	=	ignition delay time
ϕ	=	equivalence ratio

Received 21 December 2009; revision received 25 October 2010; accepted for publication 2 November 2010.

*Research Associate, Institute of Engineering Innovation, 2-11-16 Yayoi, Bunkyo-ku. Member AIAA.
†Graduate Student, Department of Chemical System Engineering, 7-3-1 Hongo, Bunkyo-ku.
‡Professor, Institute of Engineering Innovation, 2-11-16 Yayoi, Bunkyo-ku. Member AIAA.
§Graduate Student, Department of Aero Space Science, 3-1-1 Yoshinodai, Sagamihara.
¶Associate Professor, Department of Mechanical and Control Engineering, 1-1 Sensui-cho, Tobata-ku. Member AIAA.

I. Introduction

HYDROGEN attracts much attention because of its importance as a future energy resource enabling the reduction in environmental load. Although liquid rocket propulsion is currently the only practical device that uses hydrogen as a fuel, it is likely that our demand for hydrogen will rise in the future.

Several detailed chemical kinetic mechanisms of hydrogen combustion have recently been developed and are being updated by many researchers [1–6]. These models have been validated using a wide range of measurements and were generally found to be in good agreement with experimental data, including ignition delay times with shock tubes, reaction behavior in flow reactors, and laminar flame speeds. Rate constants and third-body efficiencies for many elementary reactions seem to be evident in hydrogen/oxygen systems. However, determining some rate constants characterized by high sensitivity at high pressures has remained a challenge. Among the recent kinetic models, those developed by Li et al. [2], O'Conaire et al. [3], and Konnov [4] may have more completely incorporated data from the most extensive validations. The modeling range covers temperatures from 950 to 2700 K and pressures up to 87 atm for shock-tube ignition delay times. These models were also validated against flow tube experiments at around 900 K, with pressures ranging from 0.3 to 15.7 atm and against laminar flame speeds up to a pressure of 20 atm.

A liquid rocket engine is an example of the use of hydrogen as a fuel, and it may be the first device putting hydrogen into practical use. In a typical liquid rocket engine, the pressure in the combustion chamber reaches 200 atm, which is much higher than the pressure in other popular combustion devices, such as an automobile engine or a gas turbine. To understand or predict combustion flow in a liquid rocket engine, a new detailed kinetic mechanism of an H_2/O_2 system is needed, because all models proposed thus far have not been validated under high-pressure conditions, limiting their applicability. Under such high-pressure conditions, it is very difficult to obtain the experimental data needed to determine a rate constant. Therefore, some rate constants must be determined theoretically without using

experimental data. In addition, there is no diluent in the combustion flow in a liquid rocket engine, although there are some diluents such as nitrogen or argon in many experimental measurements of flame speeds or ignition delay times. This also makes it difficult to develop a detailed kinetic model applicable to a liquid rocket engine.

Recently, chemical kinetics of high-pressure H_2 combustion have been reviewed by Law [7] and Chaos and Dryer [8]. Those reviews indicate the significance of chemical kinetics for predicting the characteristics of high-pressure H_2 combustion. Recent studies performed by Burke et al. [9–11] provide examples in which some discrepancies can be found between model predictions and experimental results for hydrogen/oxygen combustion under high-pressure conditions. In these studies, they examined the pressure dependencies of mass burning rates for hydrogen mixtures for equivalence ratios from 0.7 to 2.5 and for pressures from 1 to 25 atm. They found that under high-pressure conditions, the mass burning rate decreased as the pressure increased, while under low-pressure conditions, the mass burning rate increased as the pressure increased. Predictions of the mass burning rate based on the recently published chemical kinetic models provide almost the same results and are in good agreement with the experimental data obtained at lower pressures. On the other hand, at higher pressures, prediction results differ significantly depending on the model, and yet prediction of the mass burning rate at high pressures is crucial for the application of a kinetic model that enables us to understand the combustion flow of the hydrogen/oxygen system at high pressures. Burke et al. [11] suggested that it would be necessary to modify several rate constants in the current hydrogen combustion models in order to predict high-pressure flame properties. They also suggested the possibility that some important elementary reactions are still missing in the current hydrogen combustion mechanism.

The objective of this work, therefore, is to construct a detailed kinetic mechanism of a hydrogen/oxygen system that can be used under high-pressure and no-diluent conditions, such as a liquid rocket engine. For the purpose of applying the model at high pressures, special attention is paid to third-body recombination or dissociation reactions, which are very important in high-pressure conditions.

II. Reaction Kinetics

Table 1 shows a detailed kinetic model constructed for this study, which consists of 21 elementary reactions, including eight species of H_2, O_2, H_2O, H, O, OH, HO_2, and H_2O_2. This model was developed by improving or revising some rate constants in the previous model by Kitano et al. [27]. In developing this model, no attempt was made to adjust the rate constant in order to obtain agreement with target

Table 1 H_2/O_2 reaction mechanism (units: cm, mol, cal, K)

Reaction No.	Reaction	A	n	E_a	F_C	Efficiency parameters
R1 [12]	$OH + H_2 = H_2O + H$	2.160×10^8	1.51	3440	——	——
R2 [13]	$H + O_2 = OH + O$	1.910×10^{14}	0.0	16440	——	——
R3 [14]	$O + H_2 = OH + H$	5.080×10^4	2.67	6292	——	——
R4 [15]	$OH + HO_2 = H_2O + O_2$	2.890×10^{13}	0.0	−500	——	——
R5[a]	$H + HO_2 = H_2 + O_2$	3.660×10^6	2.09	−1450	——	——
R6 [1]	$H + HO_2 = OH + OH$	7.080×10^{13}	0.0	300	——	——
R7	$H + HO_2 = H_2O + O$	1.340×10^{13}	0.0	1340	——	——
R8 [16]	$O + HO_2 = O_2 + OH$	3.250×10^{13}	0.0	0.0	——	——
R9-A[b] [17]	$HO_2 + HO_2 = H_2O_2 + O_2$	4.200×10^{14}	0.0	12000	——	——
R9-B[b] [18]	$HO_2 + HO_2 = H_2O_2 + O_2$	1.320×10^{11}	0.0	−1192	0.5	Unity for all species
R9-B[b] [18]	$HO_2 + HO_2 + M = H_2O_2 + O_2 + M$	6.890×10^{14}	0.0	−1947	0.5	Unity for all species
R10 [14]	$OH + OH = O + H_2Oa$	4.330×10^3	2.7	−2485	——	——
R11	$H_2O_2 + H = H_2O + OH$	8.190×10^8	1.55	3455	——	——
R12-A[b] [19]	$H_2O_2 + H = HO_2 + H_2$	8.067×10^{19}	−1.574	16838	——	——
R12-B[b] [19]	$H_2O_2 + H = HO_2 + H_2$	1.042×10^{13}	0.0	6569	——	——
R13-A[b] [20]	$H_2O_2 + OH = H_2O + HO_2$	1.700×10^{18}	0.0	29407	——	——
R13-B[b] [20]	$H_2O_2 + OH = H_2O + HO_2$	2.000×10^{12}	0.0	427	——	——
R14 [16]	$H_2O_2 + O = HO_2 + OH$	6.620×10^{11}	0.0	3974	——	——
R15-1[c][20]	$H + O_2 = HO_2$	1.933×10^{12}	0.56	0.0	0.62	——
R15-1 [c][21,22]	$H + O_2 + M = HO_2 + M$	4.570×10^{18}	−1.12	0.0	0.62	——
R15-2 [20]	$H + O_2 = HO_2$	1.933×10^{12}	0.56	0.0	0.5	——
R15-2[d]	$H + O_2 + H_2 = HO_2 + H_2$	3.520×10^{18}	−0.896	0.0	0.5	——
R15-3 [20]	$H + O_2 = HO_2$	1.933×10^{12}	0.56	0.0	0.67	——
R15-3 [21,22]	$H + O_2 + N_2 = HO_2 + N_2$	1.750×10^{19}	−1.232	0.0	0.67	——
R15-4 [20]	$H + O_2 = HO_2$	1.933×10^{12}	0.56	0.0	0.5	——
R15-4[d]	$H + O_2 + O_2 = HO_2 + O_2$	1.410×10^{18}	−0.849	0.0	0.5	——
R15-5 [20]	$H + O_2 = HO_2$	1.933×10^{12}	0.56	0.0	0.81	——
R15-5 [20]	$H + O_2 + H_2O = HO_2 + H_2O$	3.630×10^{19}	−1.0	0.0	0.81	——
R15-6 [20]	$H + O_2 = HO_2$	1.933×10^{12}	0.56	0.0	0.59	——
R15-6 [21,22]	$H + O_2 + He = HO_2 + He$	3.630×10^{19}	−1.0	0.0	0.59	——
R16-1[c] [23]	$H + H + M = H_2 + M$	7.000×10^{17}	−1.0	0.0	——	$O_2 = 2.2$; $H_2O = 14.4$
R16-2 [23]	$H + H + H_2 = H_2 + H_2$	1.000×10^{17}	−0.6	0.0	——	——
R16-3 [23]	$H + H + N_2 = H_2 + N_2$	5.400×10^{18}	−1.3	0.0	——	——
R16-4 [23]	$H + H + H = H_2 + H$	3.200×10^{15}	0.0	0.0	——	——
R17	$H + OH + M = H_2O + M$	3.500×10^{22}	−2.0	0.0	——	$H_2O = 12.0$; Ar = 0.38; He = 0.38 [2]
R18 [24]	$H + O + M = OH + M$	6.750×10^{18}	−1.0	0.0	——	$H_2O = 5.0$
R19-1[c] [25]	$O + O + M = O_2 + M$	6.160×10^{15}	−0.5	0.0	——	$H_2 = 2.5$; $H_2O = 12.0$
R19-2 [25]	$O + O + Ar = O_2 + Ar$	1.890×10^{13}	0.0	−1790	——	——
R19-3 [25]	$O + O + He = O_2 + He$	1.890×10^{13}	0.0	−1790	——	——
R20-A [20]	$H_2O_2 = OH + OH$	3.000×10^{14}	0.0	48482	0.44	$H_2 = 3.0$; $O_2 = 2.2$; $H_2O = 15.0$; $N_2 = 3.0$
R20-B [26]	$H_2O_2 + M = OH + OH + M$	2.290×10^{16}	0.0	43634	——	——
R21	$O + OH + M = HO_2 + M$	3.820×10^{15}	−0.216	0.0	——	——

[a]Calculated from the canonical variational transition state theory (CVTST) rate constant of the reverse reaction in Ref. [50].
[b]Expressed as the sum of the two rate expressions.
[c]When a rate constant is declared specially for an Ar, H_2, N_2, H, O_2, H_2O, or He collision partner, the efficiency of Ar, H_2, N_2, H, O_2, H_2O, or He is set to zero when determining M for the same reaction.
[d]Evaluated in this study.

validation data, except for the rate constant of the $H + OH + M = H_2O + M$ reaction. Instead, rate constants were compiled from the most reliable values in the literature. The first key issue was to determine third-body efficiencies for H_2, O_2, and H_2O, since these efficiencies are very important and sensitive to the accuracy of the model under high-pressure and no-diluent conditions. In this section, a detailed explanation for these elementary reactions is presented.

A. $HO_2 + HO_2 = H_2O_2 + O_2$ (R9)

This reaction is important at high pressures relevant to rocket engine combustion because H_2O_2 is predominantly produced by this reaction. Hydrogen peroxide is an important chain carrier for the degenerate branching mechanism near the third explosion limit [7]. The rate constant of this reaction has unusual temperature dependence and reaches a minimum at around 500 K. In the low-temperature region (below 500 K, where the rate constant decreases with increasing temperature), pressure dependence of the rate constant is also observed because the reaction proceeds via H_2O_4 complex formation [18,28]. Although this pressure dependence has a large impact on atmospheric chemistry, its relevance to combustion chemistry is not clear. Baulch et al. [20] indicated that the rate constant is pressure independent at temperatures above 550 K. The pressure dependence of this rate constant was not included in the previous kinetic model [1–3]. However, the termolecular reaction $HO_2 + HO_2 + M = H_2O_2 + O_2 + M$ is included in Konnov's model [4]. He found that this pressure-dependent reaction could not be negligible for the prediction of shock-tube ignition delay times at high pressures and relatively low temperatures. In the present model, we also include the pressure dependence of this reaction with the fall-off behavior proposed by Atkinson et al. [18]. Since the fall-off pressure of this reaction is calculated to be around 11 atm at 1000 K by using low- and high-pressure limiting rate constants recommended by Atkinson et al., the use of a low-pressure limiting rate constant may not be adequate for high-pressure conditions.

It is also well known that the existence of H_2O accelerates this reaction significantly at low temperatures [18,29,30]. This effect of water is very important in atmospheric chemistry, but its role vanishes at temperatures above 400 K [29,30]. Therefore, the enhancement factor of H_2O on the fall-off reaction (R9-B) is not considered in the present model. The high-temperature rate constant of the reaction (R9-A), which is independent of pressure, is taken from Hippler et al. [17].

B. $H + O_2 + M = HO_2 + M$ (R15)

This reaction is most sensitive to ignition delay times near the second explosion limit, and several theoretical and experimental studies pertaining to this reaction have recently been conducted [21,22,31,32]. The high-pressure limiting rate constant of this reaction is derived from that evaluated theoretically by Troe [33], which is recommended by Baulch et al. [20] and popularly used in many other kinetic models. The low-pressure limiting rate constants for $M = H_2$, O_2, and H_2O are especially important for the present purpose. Considerable experimental data are found for $M = H_2O$, and the third-body efficiency seems to be well established. In the present model, the rate constant for $M = H_2O$ is taken from the experimental determination by Michael et al. [21], whereas experimental data for $M = O_2$ or H_2 are rather sparse.

The literature values of rate constants for $M = H_2$ [21,31–40] are depicted in Fig. 1. The low-pressure limiting rate constant of this reaction has been evaluated recently by Michael et al. [21] on the basis of the collision theory. The resulting rate constant is in good agreement with the experimental value determined by Nielson et al. [34] at room temperature and with that by Baldwin [35] at $T = 773$ K. Considering the rate constants obtained by Kochubei and Moin [36] at high temperatures ($T = 913$–1470 K), the rate constant was evaluated to be $3.52 \times 10^{18} T^{-0.896}$ cm^6 mol^{-2} s^{-1}. This expression gives slightly lower values than those recommended by Baulch et al. [16].

The low-pressure limiting rate constants for $O + H_2 + O_2$ have been both experimentally and theoretically evaluated by Michael

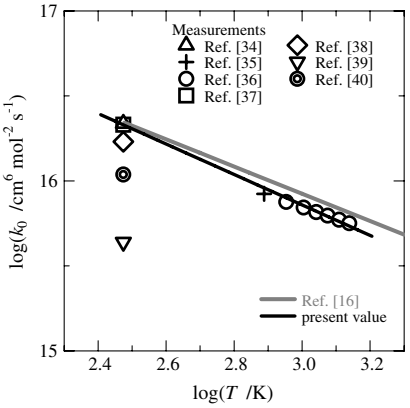

Fig. 1 The low-pressure limiting rate constant of $H + O_2 + H_2 = HO_2 + H_2$ (R15-2).

et al. [21] at $T = 298$ K and $T = 513$–697 K. These values are plotted in Fig. 2, along with other values from the literature. We evaluated rate constants at higher temperatures ($T = 1100$–1400 K) using the shock-tube ignition delay times measured by Hasegawa and Asaba [41]. The related data shown in Fig. 3 have been measured with 2% H_2 diluted in O_2. It was found that the rate constant of the $O + H_2 + O_2 = HO_2 + O_2$ reaction was very sensitive to the ignition delay times at around $T = 1200$ K, which is indicated as the point at which the slope changes around $1000/T = 0.82$ in the horizontal axis in Fig. 3. This change in slope is caused by the second explosion limit, which is determined by the competition between the reactions $H + O_2 = OH + O$ (R2) and $H + O_2 + O_2 = HO_2 + O_2$ (R15-4). Since the values for reaction R2 are well established, the rate constants for R15-4 can be evaluated by fitting the corresponding

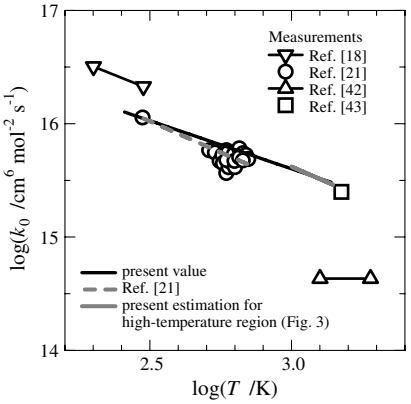

Fig. 2 The low-pressure limiting rate constant of $H + O_2 + O_2 = HO_2 + O_2$ (R15-4).

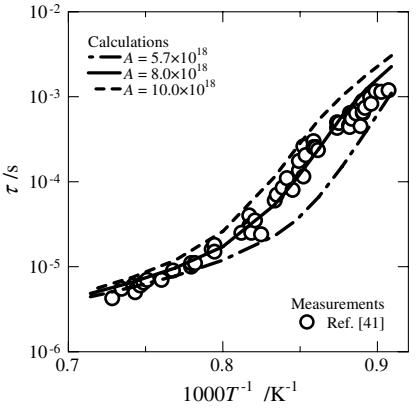

Fig. 3 Ignition delay times for various initial temperatures in $H_2/O_2 = 2/98$ mixtures at pressure of 9 atm.

ignition delay times. Calculated values with three different values of the A factor for the rate constant of R15-4 are also depicted in Fig. 3. As indicated in this figure, the low-pressure limiting rate constant of $8.0 \times 10^{18} T^{-1.094}$ cm^6 mol^{-2} s^{-1} reproduces the experimental results accurately. Figure 2 compares the low-pressure limiting rate constants obtained by Michael et al. [21] with the present results and other literature values [42–44]. The expression of $1.41 \times 10^{18} T^{-0.849}$ cm^6 mol^{-2} s^{-1} is obtained for the low-pressure limiting rate constant of $H + O_2 + O_2 = HO_2 + O_2$ (R15-4) using the present estimation and the experimental data from Michael et al. [21]. The present estimation is also in good agreement with the value proposed by Peeters and Mahnen [43] at $T = 1500$ K.

C. $H + OH + M = H_2O + M$ (R17)

This reaction is sensitive to flame speeds under high-pressure conditions [2,3]. To our knowledge, no experimental data on the high-pressure limiting rate constant or the fall-off behavior of the reaction have been reported in the literature. Sellevag et al. [31] recently theoretically evaluated the high-pressure limiting rate constant using the variable reaction coordinate TST on the basis of potential energy surfaces obtained at the CASPT2/aug-cc-pVTZ level of the theory. They also evaluated the low-pressure limiting rate constants for M = N_2 and Ar. Their values for M = Ar are slightly lower than the recommended values of Baulch et al. [20] above 1500 K, and for M = N_2, their values are two to three times lower than the recommended value. For M = H_2O, Javoy et al. [45] measured the rate constant using a shock-tube technique combined with an atomic resonance absorption spectrometry. Available data in literatures are largely scattered [18,20] and span more than an order of magnitude. In the kinetic model of Li et al. [2], they increased the A factor of this reaction recommended by Tsang and Hampson [25] by 1.7 times ($k = 3.8 \times 10^{22} T^2$ cm^6 mol^{-2} s^{-1}, for M = N_2) in order to obtain better agreement of flame speed calculation. This rate constant is in the middle of the range of recent literature values. O'Conaire et al. [3] also increased the A factor to twice the recommended value in their kinetic model. On the other hand, Konnov [4] used the rate constant calculated from the rate constant of the reverse reaction of H_2O dissociation measured by Srinivasan and Michael [46]. Temperature dependence of this rate constant is greater than the recommended rate constant by Baulch et al. [20].

To improve laminar flame predictions, we also modified the A factor of the rate constant of reaction R17 for M = N_2, recommended by Baulch et al. [20]. The resulting A factor of 3.5×10^{22} cm^6 mol^{-2} s^{-1} is essentially the same as that of Li et al. [2]. The third-body efficiencies for M = Ar, He, and H_2O are taken from Li et al. and O'Conaire et al. [3] (0.38, 0.38, and 12.0 relative to N_2, respectively). The third-body efficiencies for M = H_2 and O_2 are assumed to be the same as that for N_2.

D. $H_2O_2 + M = OH + OH + M$ (R20)

This reaction is important at pressures above the third explosion limit and is sensitive to the ignition characteristics at conditions relevant to rocket engine combustion. The dissociation of H_2O_2 and the reverse recombination has been studied frequently in theoretical modeling and detailed experimental study [20]. Under the present target conditions (pressures up to 200 atm), this reaction can be in the fall-off region. The rate constants in the fall-off region have recently been measured by Kappel et al. [26], and theoretical calculations of the high-pressure limiting rate constant have been performed by Troe and Ushakov [47]. Their theoretical fall-off curves are consistent with the experimental data of Kappel et al. [26]. Their evaluations are used in the present kinetic mechanism.

E. $H + H_2O_2$ Reactions (R11 and R12)

There are two possible exit channels for this reaction: $H_2O_2 + H = H_2O + OH$ (R11) and $H_2O_2 + H = HO_2 + H_2$ (R12). Although those reactions are less sensitive to the laminar flame speeds at pressures less than 100 atm, the values of these rate constants were found to be sensitive to the ignition delay times at high pressures relevant to liquid rocket engine combustion.

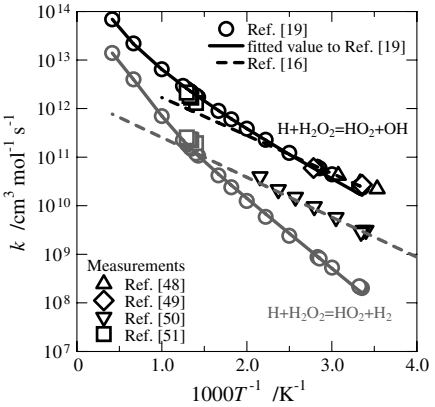

Fig. 4 Rate constants of $H_2O_2 + H = H_2O + OH$ (R12).

The rate coefficients for the overall $H_2O_2 + H$ reaction (R11 + R12) have been determined by Klemm et al. [48] and Michael et al. [49] at low temperatures and by Albers et al. [50] at $T = 294$–464 K. These authors claimed that reaction R11 dominated in terms of the rate coefficient. Although the values obtained by Klemm et al. [48] and Michael et al. [49] are in good agreement with each other, the values obtained by Albers et al. [50] are considerably lower. Baldwin and Walker [51] evaluated the rate constants of R11 and R12 at $T = 713$–773 K. These values are plotted in Fig. 4 together with the recommended values by Baulch et al. [16], which are mainly based on the results of Baldwin and Walker [51]. Note that, although the experimental values by Albers et al. [50] agree well with the recommendation of Baulch et al. [16] for reaction R12, the values of Albers et al. [50] could be the sum of the rate constants for reactions R11 and R12. Therefore, the recommended value of Baulch et al. [16] may be overestimated.

Ellingson et al. [19] recently evaluated the rate constants for reactions R11 and R12 using the canonical variational transition theory combined with high-level quantum chemical calculations of potential energy surfaces. They presented two sets of rate constants for reaction R12. One (so-called set I in [19]) is obtained with the electronic structure calculations by the MPW1B95/MG3 method, and the resulting rate constant is in good agreement with the experimental data from Albers et al. [50]. The other (set II) is based on the M05-2X/MG3S calculation, and this rate constant is in good agreement with the experimental results of Klemm et al. [48]. Although we tried both sets of rate constants for reaction R12 in the present simulations, the experimental data used in the present study to validate the mechanism ($p < 67$ atm) are insensitive to the rate constant of R12. No experimental data are available at pressures relevant to rocket engine combustion ($p > 100$ atm), where this reaction is expected to be sensitive. We employed the set II rate constant for reaction R12, which agrees well with the experimental data of Baldwin and Walker [51] and Klemm et al. [48]. This rate constant is also in good agreement with the rate constant at low temperatures recommended by Baulch et al. [16].

Reaction R11 has a higher activation barrier than that of reaction R12, and there are no reliable experimental data except those obtained by Baldwin and Walker [51] at $T = 713$–753 K. The canonical variational theory calculation of this rate constant by Ellingson et al. [19] is in good agreement with the data of Baldwin and Walker [51]; hence, this rate constant of R11 is used in the present kinetic mechanism.

F. $H + HO_2$ Reactions (R5, R6, and R7)

The reaction between H atoms and HO_2 radicals includes three dominant product channels: $H + HO_2 = H_2 + O_2$ (R5), $H + HO_2 = OH + OH$ (R6), and $H + HO_2 = H_2O + O$ (R7). Rate constants of those reactions and product branching ratios have greater sensitivities to the mass burning rates at high pressures [9–11].

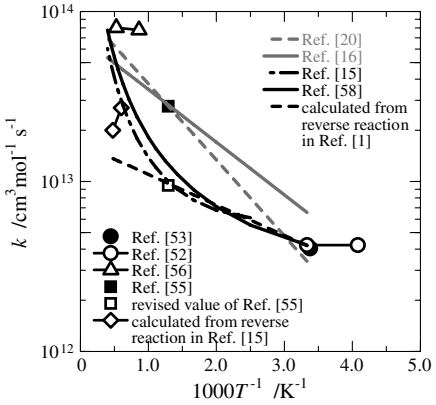

Fig. 5 Rate constants of $H + HO_2 = H_2 + O_2$ (R5).

Recent recommendations and some selected experimental data of reactions R5–R7 are shown in Figs. 5–7. Most recommendations of these reactions are based on the room temperature data of Keyser [52] and Sridharan et al. [53] and modeling studies of H_2/O_2 explosion limit data obtained by Baldwin et al. [54]. In the experiments of Keyser [52] and Sridharan et al. [53], concentrations of $O(^3P)$ and OH were monitored, and the overall rate and branching fractions were determined. The rate constants of reactions R5–R7 evaluated by the International Union of Pure and Applied Chemistry (IUPAC) Panel [55] are based on those experimental results. At higher temperatures, there are few data, and the data points are highly scattered. In general, the data of Baldwin et al. [54] are considered most reliable [16,18,25,44]. Baldwin et al. [54] determined the ratios of rate constants $k_5/k_2k_4^{1/2}$ and $k_6/k_2k_4^{1/2}$ on the basis of the second explosion limit data at $T = 773$ K. Therefore, their values of k_5 and k_6 depend of the choice of k_2 and k_4. Baldwin and Walker later revised the original values [55], and recent recommended values of k_5 and k_6 by Baulch et al. [20] were based on these revised values combined with the low-temperature data of Keyser [52] and Sridharan et al. [53], as shown in Figs. 5 and 6. On the other hand, Mueller et al. [1] also revised these rate constants using values of k_2 and k_4, used in their kinetic model. Rate constants of Mueller et al. are also adopted in the kinetic models of Li et al. [2] and O'Conaire et al. [3]. Those rate constants of reactions R5 and R6 are also depicted in Figs. 5 and 6. There are considerable differences in the rate constants of Mueller et al. [1] and Baulch et al. [20] at higher temperatures.

Michael et al. measured the rate constant of the reverse reaction R5, $H_2 + O_2 = HO_2 + H$, using a shock tube at $T =$ 1662–2097 K [15]. They also performed the canonical transition state theory (CTST) calculations for this reaction at $T = 400$–2300 K. Those rate constants are converted to the rate constant of the reverse reaction R5 combined with the equilibrium constant and are plotted in Fig. 5, together with the high-temperature data of Hidaka et al. [56]. The rate constant of R5 obtained from the CTST results can be expressed as

$$k_5 = 3.66 \times 10^6 T^{2.087} \exp(+1450/RT)(\text{units: cm, mol, cal, K}) \quad (1)$$

As can be observed in Fig. 5, this rate constant agrees quite well with the rate constant of Mueller et al. [1] at temperatures below 1000 K and with the room temperature data of Keyser [52] and Sridharan et al. [53]. The rate constants of Eq. (1) for reaction R5, together with the rate constant of R6 derived by Mueller et al. [1], are adopted in the present model.

In the kinetic models of Mueller et al. [1], Li et al. [2], and O'Conaire et al. [3], reaction R7 is not included. Baldwin et al. [54] could not separate reaction R7 from reaction R6, because these reactions are kinetically similar. The product branching fractions obtained by Keyser [52] and Sridharan et al. [53] indicated that reaction R7 is much slower than reaction R6. Day et al. [57] estimated the temperature-independent branching fraction of $k_7/k_6 = 0.1$ in their modeling study. However, Konnov [4] indicated that the sensitivities of the burning velocity to the rate constants of reactions R6 and R7 have opposite signs. Thus, these reactions are kinetically different, and both reactions should be considered in the reaction mechanism. Konnov used the temperature-independent rate constant of R7 evaluated by Baulch et al. [20]. Recommendation of the rate constant of reaction R5 by Baulch et al. is also employed in the Konnov [4] mechanism, but the rate constant of reaction R6 was taken from Baulch et al. [16] and slightly scaled up to fit the room temperature evaluation of the IUPAC Panel [18]. In the present model, the branching ratio of $k_7/k_6 = 0.1$ is assumed, and the value of k_7 is derived at $T = 773$ K from the revised value of k_6 given by Mueller et al. [1]. This value at $T = 773$ K is combined with the values of k_7 evaluated by the IUPAC Panel [18]. The resulting rate constant is expressed as

$$k_7 = 1.34 \times 10^{13} \exp(-1317/RT)(\text{units: cm, mol, cal, K}) \quad (2)$$

This evaluation is close to the recommended rate constant of Baulch et al. [16], as shown in Fig. 7.

The detailed mechanism of the $H + HO_2$ reaction is actually quite complex. Mousavipour and Saheb [58] performed high-level quantum chemical calculations (density functional theory, coupled cluster singles and doubles model (CCSD), and Gaussian-3 theory (G3) methods with the aug-cc-pVTZ basis set) of potential energy surfaces of the $H + HO_2$ reaction systems on both singlet and triplet manifolds. They investigated two different channels on the triplet surface: $H + HO_2 = H_2(^1\Sigma_g^+) + O_2(^3\Sigma_g^-)$ (R5) and $H + HO_2 = H_2O + O(^3P)$ (R7). Those two channels have activation barriers of 1.48 and 18.6 kcal/mol [CCSD (full)/aug-cc-pVTZ], respectively. They also evaluated the rate constants using the transition state theory (TST). The resulting rate constants are plotted in Figs. 5 and 7. Their rate constant of R5 is close to the rate constant of Eq. (1). The transition states on the lowest triplet surface for the $H + HO_2$ reaction were also investigated by Karkach and Osherov [59], and similar results were obtained. On the other hand, the rate constant of reaction R7 (Fig. 7) is very small because of the energy barrier. An oxygen atom is also produced on the singlet manifold by the channel

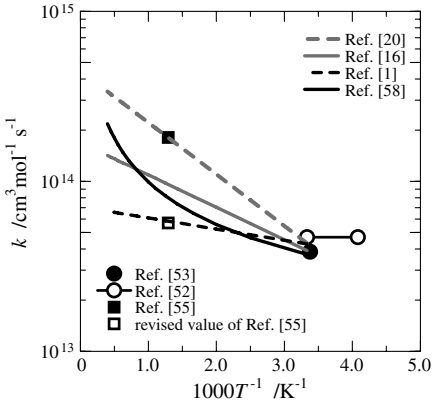

Fig. 6 Rate constants of $H + HO_2 = OH + OH$ (R6).

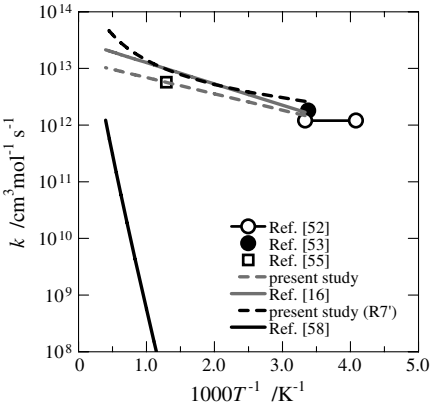

Fig. 7 Rate constants of $H + HO_2 = H_2O + O$ (R7).

of $H + HO_2 = H_2O + O(^1D)$ (R7') through the formation of energized water oxide, H_2OO*. There is no activation barrier for this channel. Their rate constant of R7', evaluated by the Rice–Ramsperger–Kassel–Marcus (RRKM) theory, is also depicted in Fig. 7. Interestingly, this rate constant is very close to the rate constant of R7 recommended by Baulch et al. [16] and, hence, close to the rate constant of Eq. (2). The implications of this will be discussed in the next section in detail. Mousavipour and Saheb [58] distinguished two different channels to produce $2OH(^2\Pi)$ (reaction R6): one is through the formation of HOOH*, and the other is through the formation of H_2OO*. The RRKM rate constant as a sum of these two channels is compared with other rate constants of reaction R6 in Fig. 6. This rate constant agrees well with the evaluation of Mueller et al. [1] at lower temperatures, but it gives higher values at higher temperatures. It is found that the adoption of this RRKM rate constant in the present model results in faster mass burning rates at high pressures. They found one more singlet channel to produce $H_2 + O_2(^1\Delta)$ with the activation barrier of 19 kcal/mol [CCSD (full)/aug-cc-pVTZ]. This channel is slow compared with other reaction paths and can therefore be neglected.

G. $OH + HO_2 = H_2O + O_2$ (R4)

This reaction also has high sensitivity at high-pressure conditions around the third explosion limit, since this reaction acts as termination. Hippler et al. [60] found the deep and narrow rate constant minimum close to 1250 K. They suggested that the anomalous temperature dependence of this reaction was caused by the formation of an intermediate complex. This deep and unusually narrow rate constant minimum was confirmed by Kappel et al. [26], but the minimum was observed near 1000 K. Keyser [61] showed that reaction R4 exhibited no pressure dependence at pressures up to 1000 atm and the temperature from 254 to 382 K.

In the kinetic models of Li et al. [2] and O'Conaire et al. [3], this unusual temperature dependence was not considered, and they employed the rate constant recommended by Baulch et al. [16], which was based on the low-temperature measurement of Keyser [61]. The high-temperature part of the measurements of Hippler et al. [60] was adopted by Baulch et al. [20] as a recommendation over the range 1300–2000 K. Konnov [4] approximated the rate constant as a sum of two expressions of the low-temperature part [16] and the high-temperature part [20]. The approximation adopted by Konnov [4] does not reproduce the deep and narrow rate constant minimum observed by Hippler et al. [60] or Kappel et al. [26]. Sivaramakrishnan et al. [62] recently proposed a new parameterization for the rate of reaction R4. They fitted the rate constant over a wide range of experimental data using the sum of five Arrhenius expressions. This expression was further refined by Chaos and Dryer [8].

Recently, Srinivasa et al. [63] measured the rate constant of R4 at $T = 1200$–1700 K. They did not observe the clear temperature dependence. Hong et al. [64] determined the rate constant of R4, based on the measurement of the reverse rate constant at $T = 1600$–2200 K, using a shock tube. Their values of the rate constants, as well as those of Srinivasa et al. [63], are in good agreement with the extrapolations of the recommended rate constant of Baulch et al. [16], based on the low-temperature values. Relatively high positive activation energy ($\sim$17.5 kcal/mol) at $T > 1300$ K was assigned in the recommendation by Baulch et al. [20], but no such strong positive temperature dependence was observed in those two studies.

Gonzalez et al. [66] conducted ab initio calculations of the $OH + HO_2$ reaction, both on the singlet [65] and triplet [66] potential energy surfaces. They concluded that the reaction proceeds predominantly on the triplet surface as an H atom abstraction reaction. It was found that the hydrogen bond in the complex H_2O–O_2 is too weak to produce significant pressure dependence, and the reaction is not controlled by the transition state on the triplet energy surface. They also estimated the thermal rate constant of the target reaction based on the adiabatic theory and slight negative temperature dependence, which agrees with the recommended values by the early review of Baulch et al. [16].

Considering those recent high-temperature determinations of the rate constants [63,64] and the theoretical consideration of Gonzalez et al. [66], we adopted the early recommendation of Baulch et al. [16] for the rate constant of this reaction.

H. $H + OH + M = HO_2 + M$ (R21)

Konnov [4] revealed that this reaction was not included in previous kinetic models [1–5]. Burke et al. [11] demonstrated that this reaction can reduce the predicted mass burning rate at pressures higher than 10 atm if its rate constant is larger than 10^{16} cm^6 mol^{-2} s^{-1}. Since pressures in our target condition are ranging up to 200 atm, this reaction can be important and is included in the present model. The data on the rate constant of this reaction are sparse. To the best of our knowledge, no experimental data were reported in the literature. Germann and Miller [67] calculated the rate constant of this reaction using the flux–flux autocorrelation function. This recombination reaction competes with the other exit channel to produce $H + O_2$, the reverse reaction R2. At lower pressures, the reaction $OH + O = H + O_2$ (R2) dominates reaction R21. According to the results of Germann and Miller, the fall-off pressure of reaction R21 at $T = 500$ K is much higher than 1000 atm. Therefore, we assume this reaction is in the low-pressure limit and the rate constant of reaction R2 (hence, that of R21) is independent of pressure. By assuming the temperature dependence of AT^n for the low-pressure limiting rate constant of reaction R21, we evaluated the following rate constant based on the result of Germann and Miller: $k_{21} = 3.82 \times 10^{15} T^{-0.22}$ cm^3 mol^{-2} s^{-1}. Since there are no experimental data for the validation of this rate constant, this rate constant should be considered as tentative.

III. Results and Discussion

To confirm the accuracy of the present kinetic model, calculation results were compared with experimental results of ignition delay times and flame speeds. For comparison, calculations using the kinetic models of Li et al. [2], O'Conaire et al. [3], and Konnov [4] are also performed. All calculations were performed using CHEMKIN 4.1 [68].

A. Ignition Delay Times with Shock Tubes

Hydrogen self-ignition characteristics in mixtures with oxygen and the inert gas Ar were extensively studied using shock tubes. In the present work, high-pressure measurements of shock-tube delay times are used for the validation. Petersen et al. [69] measured ignition delay times in stoichiometric $H_2/O_2/Ar$ mixtures based on the maximum slope of the OH concentration profile. The high-pressure condition of this work is expected to be a valuable benchmark for validation of kinetic models. Figure 8 shows the comparison of experimental data together with ignition delay times

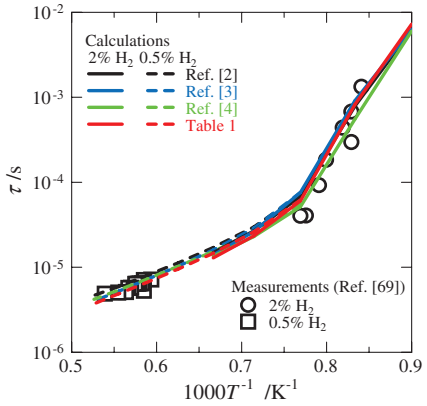

Fig. 8 Ignition delay times for two kinds of $H_2/O_2/Ar$ mixtures under stoichiometric conditions at 33 atm.

calculated by kinetic models of Li et al. [2], O'Conaire et al. [3], Konnov [4], and the present study. The ignition delay time in the modeling is defined as the moment when the temperature first exceeds the initial temperature by 50 K. As can be seen in the figure, results of all four models are very similar and in good agreement with the experimental data. Sensitivity analysis shows that the most sensitive reaction above 1300 K is the chain branching reaction R2, as expected. Although different expressions of Arrhenius parameters are employed in these models, their rate constant values are almost identical in this temperature range. On the other hand, reaction R2 and the chain termination reaction R15 are most sensitive below 1300 K. These two reactions define the second explosion limit. At temperatures between 1200 and 1300 K, reactions R5 and R6, together with other chain reactions R3, R1, and H_2O_2 reactions (R12), have little sensitivity to the ignition delay times. Reactions R5 (chain termination) and R6 (chain branching, if HO_2 is assumed to be rather inactive), together with reactions R2 and R15, define the extended explosion limit [1,70]. The temperatures of the second explosion limit at $p = 33$ atm, defined by the relation $2k_2/k_{15}[\mathrm{M}] = 1$ in those four models, are 1287, 1285, 1243, and 1247 K in Li et al. [2], O'Conaire et al. [3], Konnov [4], and the present model, respectively. These differences in the second explosion limit temperatures result from the differences in the rate constants of R15-1 for M = Ar used in each model. Despite these differences, the inflection points of ignition delay times in Fig. 8, obtained by the four models, are very identical. This is because the differences in the rate constant of R15 are compensated for by the differences in the rate constants of other reactions (especially another termination reaction R5) in these models. Therefore, the agreement between the models in Fig. 8 is rather accidental.

Slack [70] measured ignition delay times in stoichiometric H_2/air mixtures at a pressure of 2 atm behind a reflected shock wave. The ignition delay times were defined as the time between the reflected shock pressure rise and the maximum rate of change of the UV emission of OH. Identical delay times were also defined as a rapid rise in pressure signal or as the onset of infrared emission of H_2O. The ignition delay in the modeling was defined as the time when the temperature first reached a value equal to the initial one plus 50 K. Vibrational relaxation time of N_2 was not considered in the simulation, as in the previous modeling studies [3,5]. Results are shown in Fig. 9. Model predictions of the mechanisms of Li et al. [2], O'Conaire et al. [3], and Konnov [4] are very close and agree well with the experimental data, while the present mechanism significantly overpredicts ignition delays below 1025 K. This temperature is close to the second explosion limit temperature, and the calculated ignition delay times are extremely sensitive to the rate constant of reaction R15. Bhaskaran et al. [71] also measured ignition delay times in stoichiometric $H_2/O_2/N_2$ mixtures at 2.5 atm. They monitored visible emissions behind a reflected shock wave, and the ignition delay time was defined as the peak time of the emission. Comparisons with modeling predictions are shown in Fig. 10. The same definition of the ignition delay as used in the calculation of

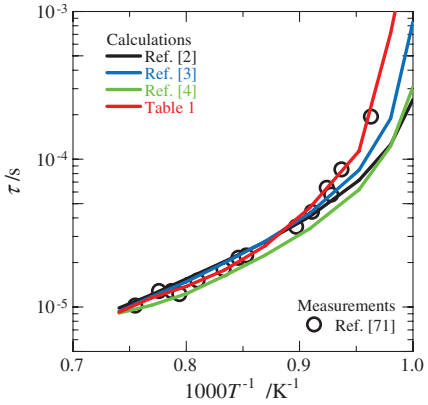

Fig. 10 Comparison of model predictions with shock-tube ignition delay times of 22.59% H_2 + 14.79% O_2, balance N_2, at 2.5 atm.

Fig. 9 is used in this case. Although the experimental conditions of Slack (Fig. 9) and Bhaskaran et al. [71] (Fig. 10) are quite similar, prediction of the present model at temperatures lower than the second explosion temperature is closer to the experimental data.

We also examined the ignition delay times against the experimental data by Catherina et al. [72]. They measured the ignition delay times of the shock heated $H_2/O_2/H_2O/Ar = 6/3/5/86$ mixture at $p = 4$ atm. The calculation results and experimental data are shown in Fig. 11. In the experiment, the intensity of the UV emission of OH at 307 nm was monitored to define the ignition delay time behind a reflected shock wave. The ignition delay time in the model prediction is defined as the peak of the product of H and O atom concentrations, [H][O], since this quantity was expected to be proportional to the UV emission of OH [72]. Figure 11 shows that the four kinetic models are in reasonable agreement with the experimental data. The model predictions below the temperature of the second explosion limit of around 1150 K are different from each other but within the scatter of the experimental data. The two data points at temperatures 1369 and 1485 K are considerably longer than the model predictions. The reason for this discrepancy is not clear. The ignition delay times at these temperatures, mainly determined by the rate constant of reaction R2 and the model predictions in Figs. 8–10, are in good agreement with the experimental data at a high-temperature range. Therefore, the origin of this discrepancy is not expected to be the chemical kinetic factor.

B. Flame Speed in Hydrogen/Oxygen/Diluents Mixtures

Figure 12 shows the measured and calculated laminar flame speeds in hydrogen/air mixtures as a function of the stoichiometric coefficient at a standard state of initial temperature and pressure. Although there is an enormous body of data for the flame speed at ambient pressure, the experimental results obtained by Dowdy et al. [73], Aung et al. [74], Tse et al. [75], and Kwon et al. [76] are plotted

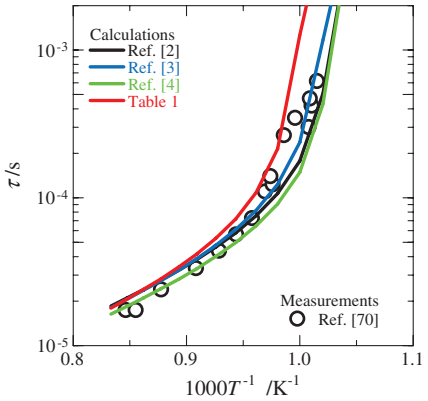

Fig. 9 Comparison of model predictions with shock-tube ignition delay times of stoichiometric H_2/air mixture at 2 atm.

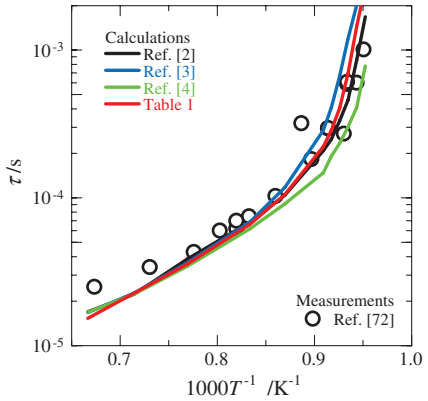

Fig. 11 Ignition delay times in $H_2/O_2/H_2O/Ar = 6/3/5/86$ mixtures at 4 atm.

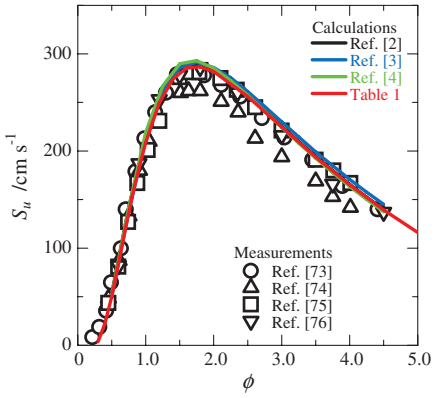

Fig. 12 Laminar flame speed for various equivalence ratios of H_2/Air mixtures at normal pressure and initial room temperature.

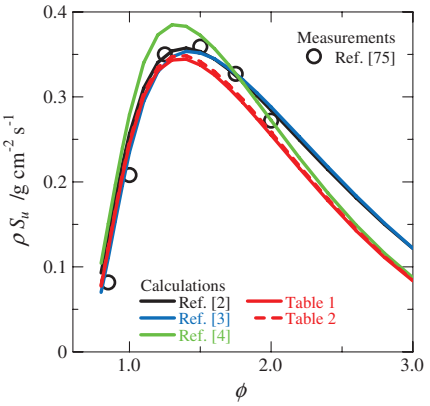

Fig. 14 Mass burning rates for $H_2/O_2/He$ flames, $O_2/H_2 = 1/11.5$, at 20 atm.

in Fig. 12 as representative data for the unstretched laminar flame speed. In CHEMKIN, a Soret effect is considered in the model predictions with a multicomponent transport option. Calculated flame speeds by the four models are almost identical, and model predictions are in good agreement with the experimental results of Dowdy et al. [73], Kwon and Faeth [76], and Tse et al. [75]. Sensitivity analysis shows that the chain branching reactions R1, R2, and R3 have high positive sensitivities. Rate constants of those reactions in four kinetic models are very similar, and resulting flame speeds are insensitive to the difference in those kinetic models. Other sensitive reactions to the flame speed are the recombination reactions R17 and R15 (M = N_2, H_2, and H_2O) and HO_2 reactions R5, R6, and R4.

The difference in mass burning rates among model predictions increases at higher pressures. Figures 13 and 14 show the comparison of unstretched laminar mass burning rates as a function of fuel equivalence ratio for H_2/O_2/He flames at pressures of 10 and 20 atm, measured by Tse et al. [75] with those of model predictions. At $p = 10$ atm, predictions of the Konnov model [4] around $\phi = 1.2$ slightly overestimate the burning rate, but predictions of the four models agree reasonably well with the experimental data, especially for the fuel-lean mixtures. Model predictions of the mass burning rates for fuel-rich mixtures differ slightly in each model, and these differences increase at 20 atm. The model predictions of Li et al. [2] and O'Conaire et al. [3] are almost identical and agree quite well with the experimental data. Mass burning rates calculated by the present model are slower than the experimental values at $\phi > 1.2$. In the fuel-rich conditions at $p = 20$ atm, reactions R2 and R6 have high positive sensitivities and reaction R7 has the highest negative sensitivity. Differences in model predictions in fuel-rich conditions are mainly caused by the difference in the value of the rate constant of R7 used in each model.

Recently, Burke et al. extensively studied the pressure and flame temperature dependencies of mass burning rates for H_2/O_2/diluent [9,10] and H_2/O_2/CO/diluent [11] mixtures. They compared their experimental results with various kinetic models in the literature, including models of [1–5]. They found that all the kinetic models tested yield predictions in good agreement with experimental data for low pressures ($p < 10$ atm), but none of the models predict the observed pressure dependence of the mass burning rate at higher pressures. They also performed extensive simulations with sensitivity analysis. According to their analysis [11], the sensitivities of mass burning rates to elementary rate constants increase considerably with pressure, and the high sensitivities at high pressures amplify the effects of uncertainties in rate constants. Validation against these high-pressure flame data is very important for the development of a model, since the high-pressure flame targets provide a stronger constraint on the rate constants. In Figs. 15 and 16, predictions of the present model are compared with the experimental data and with predictions of other kinetic model in [2–5]. The present model overestimates the maximum mass burning rate by 15% for a lean mixture of $\phi = 0.7$ (Fig. 15), while model predictions of Davis et al. [5] and O'Conaire et al. [3] agree quite well with the experimental results [10]. On the basis of the sensitivity analysis for the flame speed, Burke et al. [11] showed that competing channels of the H + O_2 and H + HO_2 reactions for the consumption of H atom, together with OH + H_2 and OH + HO_2 reactions for OH consumption, are responsible for the decrease in mass burning rates as pressure increases above 10 atm. In the present study, simulations were performed to extend the experimentally studied conditions to the rocket engine conditions up to 100 atm, as shown in Fig. 15. Although model predictions are largely different at pressures higher than 10 atm, all models predict a minimum mass burning rate at around 40–60 atm. To understand the chemical kinetic origin of this minimum, normalized sensitivities of flame speed to A factors are calculated by the present mechanism, and the results are shown in Fig. 17. As already described by Burke et al. [9,11], reactions R1, R2, R3, and R6 have high positive sensitivities as chain branching

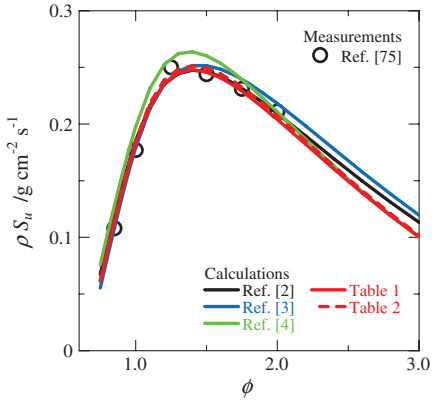

Fig. 13 Mass burning rates for $H_2/O_2/He$ flames, $O_2/H_2 = 1/11.5$, at 10 atm.

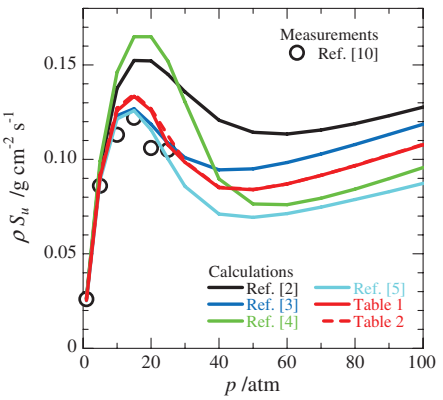

Fig. 15 Mass burning rates as a function of pressure for $H_2/O_2/He$ flames, $\phi = 0.7$, $O_2/He = 1/9.25$.

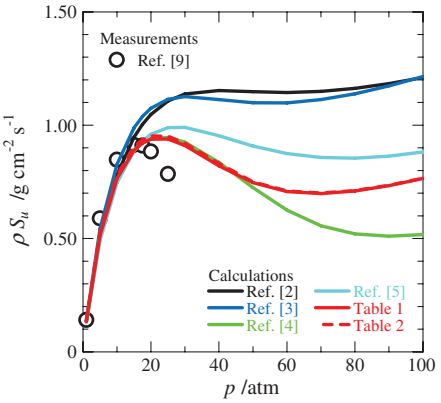

Fig. 16 Mass burning rates as a function of pressure for $H_2/O_2/Ar$ flames, $\phi = 2.5$, $O_2/Ar = 1/9.5$.

reactions, while reactions R15 (M = H_2O and He), R4, and R5 have negative sensitivities as chain termination reactions at pressures lower than 50 atm. At pressures higher than 50 atm, the absolute sensitivities of most reactions are decreasing, except those for reactions R9 and R20. Production of H_2O_2 and its decomposition constitutes a degenerate branching, and those reactions are responsible for the slow increase in mass burning rates at increasing pressure $p > 50$ atm.

Mass burning rates for a rich $H_2/O_2/Ar$ mixture ($\phi = 2.5$) are compared with experimental data in Fig. 16 and sensitivities of flame speed are depicted in Fig. 18. The maximum mass burning rate can be well reproduced by the present model, as well as by the models of Konnov [4] and Davis et al. [5]. However, none of the models (including the present mechanism) can reproduce the experimental rapid decrease of the mass burning rates above 17.5 atm. Sensitivity analysis shown in Fig. 18 indicates that the chain branching steps of R2 and R6 have very high positive sensitivities, while radical recombination reactions R15 (M = H_2O, H_2, and Ar), R16, and R17, together with the termination reaction R5, have high negative sensitivities at pressures between 10 and 50 atm. Hence, the

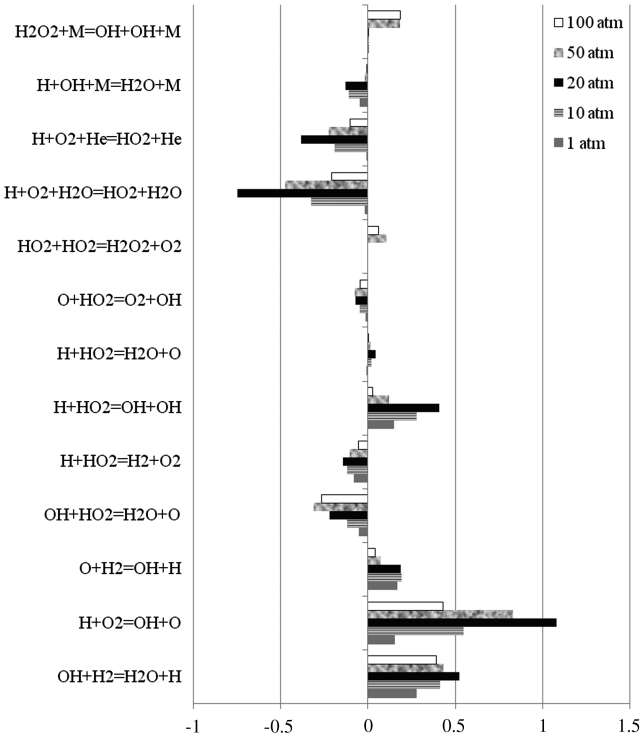

Fig. 17 Sensitivity of mass burning rate to *A* factors of elementary rates for $H_2/O_2/He$ flames of equivalence ratio 0.7 with flame temperature of 1600 K (same conditions as Fig. 15).

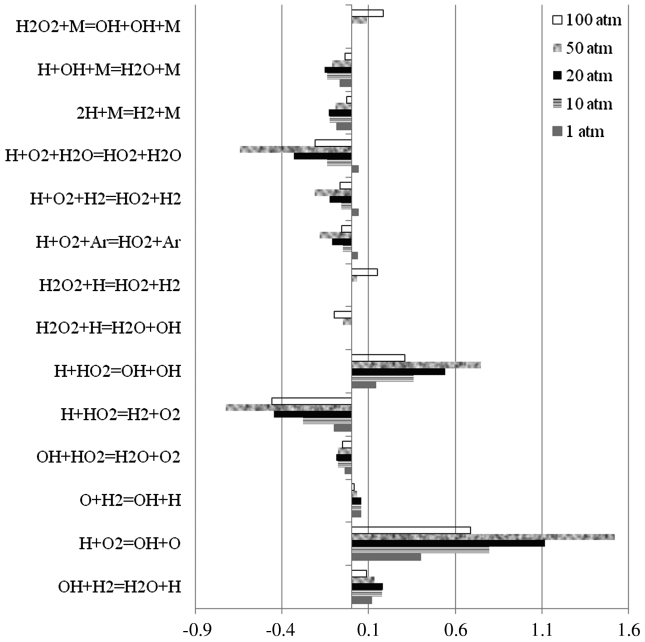

Fig. 18 Sensitivity of mass burning rate to *A* factors of elementary rates for $H_2/O_2/Ar$ flames of equivalence ratio 2.5 with flame temperature of 1600 K (same conditions as Fig. 16).

branching ratio of reactions R5 and R6 is very important for the precise prediction of the mass burning rates at this pressure range. It is also noted that the H_2O_2 reactions R11, R12, and R20 play an important role at pressures higher than 50 atm.

C. Missing Reaction

Burke et al. [11] argued that one or more elementary reactions that could be important in high-pressure H_2 flame are possibly not included in the kinetic models of H_2 combustion, as mentioned in the previous section. One candidate for the missing reaction is the $H + OH + M = HO_2 + M$ reaction. This reaction is a part of a chemical activation reaction that proceeds via a formation of stable intermediate HO_2*, and this reaction is included in the present mechanism. The impact of this reaction is small for the shock-tube ignition delay data and for the mass burning rates examined in the present study. With the present value of the rate constant, it is found that the mass burning rate decreases by about 4% by the inclusion of this reaction at $p = 10$–15 atm for a $\phi = 0.7$ mixture (Fig. 15). The mass burning rates are almost equal, both with and without this reaction, for a $\phi = 2.5$ mixture (Fig. 16). However, the accuracy of the present rate constant is not clear, and experimental data are required to confirm the rate constant.

The reaction $H + HO_2$ also proceeds via the formation of energized HOOH* or H_2OO* intermediates on the singlet surface, as discussed in the previous section. If the rate of the collisional stabilization can compete with the rate of other exit channels, the reaction $H + HO_2 + M = H_2O_2 + M$ has to be included in the model. Mousavipour and Saheb [58] calculated the rate constant of this reaction on the basis of RRKM theory. They evaluated the rate of H_2O_2 production as a sum of two different channels: $H + HO_2 \rightarrow HOOH* \rightarrow H_2O_2$ and

$$H + HO_2 \rightarrow H_2OO* \rightarrow HOOH* \rightarrow H_2O_2$$

The resulting bimolecular rate constant at 1 atm is almost temperature independent and is on the order of 10^9 cm^3 mol^{-1} s^{-1}. Therefore, this reaction is much slower than other channels R5, R6, and R7, even at 100 atm.

Troe [77] showed that the complex-forming bimolecular reactions often exhibit unusual temperature and pressure dependence, and several elementary reactions involved in the H_2 combustion mechanism are the complex-forming reactions, such as $O + OH \rightarrow$

Table 2 Reactions of $O(^1D)$ (units: cm, mol, cal, K)

Reaction No.	Reaction	A	n	E_a
R7'	$H + HO_2 = H_2O + O(^1D)$	1.340×10^{13}	0.0	1340
R22 [82]	$O(^1D) + H_2 = OH + H$	6.625×10^{13}	0.0	0
R23 [83]	$O(^1D) + H_2O = OH + OH$	7.005×10^{13}	0.0	−119
R24 [a] [82]	$O(^1D) + M \rightarrow O + M$	2.000×10^{11}	0.0	0.0
R25 [82]	$O(^1D) + O_2 \rightarrow O + O_2$	1.987×10^{13}	0.0	−109
R26 [82]	$O(^1D) + N_2 \rightarrow O + N_2$	1.295×10^{13}	0.0	−298
R27 [82]	$O(^1D) + H_2O \rightarrow O + H_2O$	2.000×10^{13}	0.0	−100

[a]When a rate constant is declared specially for an O_2, N_2 or H_2O collision partner, the efficiency of O_2, N_2, or H_2O is set to zero when determining M for the same reaction.

$HO_2* \rightarrow H + O_2$, $H + HO_2 \rightarrow HOOH*$, and $H_2OO* \rightarrow OH + OH$, as mentioned previously. Rate constants for reactions R4, R9, and R13 show strong non-Arrhenius temperature dependence, and those reactions are also believed to proceed via the complex-formation processes: $OH + HO_2 \rightarrow H_2O_3* \rightarrow H_2O + O_2$ (R4), $HO_2 + HO_2 \rightarrow H_2O_4* \rightarrow H_2O + O_2$ (R9), and

$$OH + H_2O_2 \rightarrow H_3O_3* (HO_2 - H_2O* [73])$$
$$\rightarrow H_2O + HO_2 \quad (R13)$$

Although the collisional stabilization of these energized complexes are not analyzed in detail, and their impact to the high-pressure combustion is not clear, the significant effects of these stabilization reactions at high temperatures are not expected because of weak bond energies in these complexes of H_2O_3*, H_2O_4*, and H_3O_3*.

Another possibility for the missing reaction is the formation of electronically excited species. Skrebkov et al. [78,79,81] and Skrebkov and Karkach [80] included the electronically excited $OH* (^2\Sigma^+)$, $O(^1D)$, and $O_2* (^1\Delta)$ in their kinetic model of H_2 combustion. According to the quantum chemical calculations of Mousavipour and Saheb [58], $O(^1D)$ and $O_2* (^1\Delta)$ are produced by the $H + HO_2$ reaction on the singlet potential energy surface. The channel to produce $H_2 + O_2* (^1\Delta)$ has a relatively high energy barrier (19 kcal/mol), and the channel of $H_2O + O(^1D)$ (reaction R7') proceeds via the formation of H_2OO*, without any potential barrier, and the rate constant of this reaction is in good agreement with the rate constant of the reaction $H + HO_2 = H_2O + O$ (R7) (Fig. 7). Although there is no experimental evidence for the production of $O(^1D)$ in the $H + HO_2$ reaction, its production can have significant impact on the characteristics of H_2 combustion because of its high reactivity. It is well known that the rates of $O(^1D) + H_2 = OH + H$ and $O(^1D) + H_2O = OH + OH$ are nearly equal to the collision rate. These reactions compete with collisional deactivation processes to produce ground state O atom, $O(^3P)$. The collisional deactivation to $O(^3P)$ is the spin-forbidden process if the collision partner is in a singlet manifold and the deactivation of $O(^1D)$ by noble gases is slow. On the other hand, the collisional quenching by ground state O_2 and H_2O is known to be very fast. To check the impact of $O(^1D)$ production, simulations with these reactions are performed. The reactions included in the simulations are listed in Table 2. The rate constant of reaction R7' is assumed to be the same as that of reaction R7 [Eq. (2)]. The inclusion of these reactions does not change the ignition delay times in shock-tube experiments examined in this study. This is because reaction R7 (and hence R7') has negligible sensitivity to the shock-tube ignition delay times. Mass burning rates calculated with reactions in Table 2 are included in Figs. 13–16. As shown in these figures, variations in mass burning rate by inclusion of these reactions are very small. Based on these results, it is concluded that the production of $O(^1D)$ by reaction R7' has minor impact on the ignition delay times and mass burning rates at the conditions tested in the present study.

IV. Conclusions

In the present study, several rate constants were updated in the kinetic mechanism for H_2 combustion on the basis of experimental and theoretical information for each elementary reaction. Particular attention was paid to reactions important for high-pressure conditions, including the third-body efficiencies of the $H + O_2 + M$ reaction and channel-specific rate constants of $H + H_2O_2$ and $H + HO_2$ reactions. Model predictions of the present model, as well as the models proposed by Li et al. [2], O'Conaire et al. [3], and Konnov [4], were compared with several shock-tube ignition delay data and the mass burning rate of unstretched flame. All kinetic models predicted the shock-tube ignition delay times reasonably well. Predictions of each model were almost identical for ignition delay times obtained with highly diluted conditions and agreed well with the experimental data, as shown in Fig. 8. Predictions of these kinetic models were also very close to each other for unstretched H_2/air atmospheric flame speeds (Fig. 9). However, none of the models tested in the present study could predict the high-pressure mass burning rates obtained by Burke et al. [9–11], as shown in Figs. 15 and 16. The pressure dependence of the mass burning rate at $\phi = 0.7$ was correctly predicted by the model of O'Conaire et al. [3] and Davis et al. [5], and the present model also agreed reasonably well with experimental data. On the other hand, the mass burning rates at pressures higher than 10 atm for $\phi = 2.5$ could not be predicted accurately by any of the models tested in the present study, although the maximum burning rate was correctly predicted by the model of Konnov [4], Davis et al. [5], and the present model.

The role of chemical activation reactions for high-pressure H_2 combustion was discussed to improve the model performance. The collisional stabilization of the energized molecules in the chemical activation reactions could be important. Examples of potentially important reactions are $H + OH = HO_2*$ and the competition between the decomposition and stabilization of HO_2*, $HO_2* \rightarrow H + O_2$, and $HO_2 * + M \rightarrow HO_2 + M$. More extensive experimental and theoretical studies are open for future investigations for this and other chemical activation reactions involved in the H_2 combustion. The role of the production of electronically excited species were also discussed, and it was found that the high-pressure mass burning rates of H_2 combustion are not affected by the production of $O(^1D)$ by reaction R7'.

To obtain better performance of the model prediction for the high-pressure combustion of H_2, more precise values of the rate constants are essential for the following reactions: $H + OH + M = H_2O + M$, $O + OH + M = HO_2 + M$, channel-specific rate constants for $H + HO_2$, and the temperature dependence of the $OH + HO_2 = H_2O + O_2$ reaction.

Acknowledgments

This study was supported by KAKENHI 19760572, a Grant-in-Aid for Young Scientists (B) by the Ministry of Education, Culture, Sports, Science, and Technology. This study was also partially supported by KAKENHI 19360092, a Grant-in-Aid for Scientific Research (B) by the Japan Society for the Promotion of Science.

References

[1] Mueller, M. A., Kim, T. J., Yetter, R. A., and Dryer, F. L., "Flow Reactor Studies and Kinetic Modeling of the H_2/O_2 Reaction," *International Journal of Chemical Kinetics*, Vol. 31, No. 2, 1999, pp. 113–125. doi:10.1002/(SICI)1097-4601(1999)31:2<113::AID-KIN5>3.0.CO;2-0

[2] Li, J., Zhao, Z., Kazakov, A., and Dryer, F. L., "An Updated Comprehensive Kinetic Model of Hydrogen Combustion," *International Journal of Chemical Kinetics*, Vol. 36, No. 10, 2004, pp. 566–575. doi:10.1002/kin.20026

[3] O'Conaire, M. O., Curran, H. J., Simmie, J. M., Pitz, W. J., and Westbrook, C. K., "A Comprehensive Modeling Study of Hydrogen Oxidation," *International Journal of Chemical Kinetics*, Vol. 36, No. 11, 2004, pp. 603–622. doi:10.1002/kin.20036

[4] Konnov, A. A., "Remaining Uncertainties in the Kinetic Mechanism of Hydrogen Combustion," *Combustion and Flame*, Vol. 152, No. 4, 2008, pp. 507–528. doi:10.1016/j.combustflame.2007.10.024

[5] Davis, S. G., Joshi, A. V., Wang, H., and Egolfopoulos, F., "An Optimized Kinetic Model of H_2/CO Combustion," *Proceedings of the*

Combustion Institute, Vol. 30, No. 1, 2005, pp. 1283–1292.
doi:10.1016/j.proci.2004.08.252

[6] Saxena, P., and Williams, F. A., "Testing a Small Detailed Chemical-Kinetic Mechanism for the Combustion of Hydrogen and Carbon Monoxide," *Combustion and Flame*, Vol. 145, Nos. 1–2, 2006, pp. 316–323.
doi:10.1016/j.combustflame.2005.10.004

[7] Law, C. K., "Propagation, Structure, and Limit Phenomena of Laminar Flames at Elevated Pressures," *Combustion Science and Technology*, Vol. 178, Nos. 1–3, 2006, pp. 335–360.
doi:10.1080/00102200500290690

[8] Chaos, M., and Dryer, F. L., "Syngas Combustion Kinetics and Applications," *Combustion Science and Technology*, Vol. 180, No. 6, 2008, pp. 1053–1096.
doi:10.1080/00102200801963011

[9] Burke, M. P., Chaos, M., Dryer, F. L., and Ju, Y., "Non-Monotonic Pressure Dependence in Laminar Mass Burning Rates for Hydrogen Flames," 47th AIAA Aerospace Sciences Meeting Including The New Horizons Forum and Aerospace Exposition, Orlando, FL, AIAA Paper 2009-0990, 5–8 Jan. 2009.

[10] Burke, M. P., Dryer, F. L., and Ju, Y., "Negative Pressure Dependence of High Pressure Burning Rates of H_2/O_2 Flames at Lean Conditions," 48th AIAA Aerospace Sciences Meeting Including the New Horizons Forum and Aerospace Exposition, Orlando, FL, AIAA, Paper 2010-0776, 4–7 Jan. 2010.

[11] Burke, M. P., Chaos, M., Dryer, F. L., and Ju, Y., "Negative Pressure Dependence of Mass Burning Rates of $H_2/CO/O_2$/Diluent Flames at Low Flame Temperatures," *Combustion and Flame*, Vol. 157, No. 4, 2010, pp. 618–631.
doi:10.1016/j.combustflame.2009.08.009

[12] Michael, J. V., and Sutherland, J. W., "Rate Constant for the Reaction of H with H_2O and OH with H_2 by the Flash Photolysis-Shock Tube Technique over the Temperature Range 1246–2297 K," *Journal of Physical Chemistry*, Vol. 92, No. 13, 1988, pp. 3853–3857.
doi:10.1021/j100324a035

[13] Pirraglia, A. N., Michael, J. V., Sutherland, J. W., and Klemm, R. B., "A Flash Photolysis-Shock Tube Kinetic Study of the H Atom Reaction with O_2:$H + O_2 = OH + O$ (962 K $< T <$ 1705 K) and $H + O_2 + Ar = HO_2 + Ar$ (746 K $< T <$ 987 K)," *Journal of Physical Chemistry*, Vol. 93, No. 1, 1989, pp. 282–291.
doi:10.1021/j100338a058

[14] Michael, J. V., "Measurement of Thermal Rate Constants by Flash or Laser Photolysis in Shock Tubes: Oxidations of H_2 and D_2," *Progress in Energy and Combustion Science*, Vol. 18, No. 4, 1992, pp. 327–347.
doi:10.1016/0360-1285(92)90004-K

[15] Michael, J. V., Sutherland, J. W., Harding, L. B., and Wagner, A. F., "Initiation in H_2/O_2: Rate Constants for $H_2 + O_2 = H + HO_2$ at High Temperature," *Proceedings of the Combustion Institute*, Vol. 28, No. 2, 2000, pp. 1471–1478.
doi:10.1016/S0082-0784(00)80543-3

[16] Baulch, D. L., Cobos, C. J., Cox, R. A., Esser, C., Frank, P., Just, T., Kerr, J. A., Pilling, M. J., Troe, J., Walker, R. W., and Warnatz, J., "Evaluated Kinetic Data for Combustion Modelling," *Journal of Physical and Chemical Reference Data*, Vol. 21, No. 3, 1992, pp. 411–734.
doi:10.1063/1.555908

[17] Hippler, H., Troe, J., and Willner, J., "Shock Wave Study of the Reaction $HO_2 + HO_2 \rightarrow H_2O_2 + O_2$: Confirmation of a Rate Constant Minimum Near 700 K," *Journal of Chemical Physics*, Vol. 93, No. 3, 1990, pp. 1755–1760.
doi:10.1063/1.459102

[18] Atkinson, R., Baulch, D. L., Cox, R. A., Crowley, J. N., Hampson, R. F., Hynes, R. G., Jenkin, M. E., Rossi, M. J., and Troe, J., "Evaluated Kinetic and Photochemical Data for Atmospheric Chemistry: Volume I, Gas Phase Reactions of O_x, HO_x, NO_x and SO_x Species," *Atmospheric Chemistry and Physics*, Vol. 4, No. 6, 2004, pp. 1461–1738.
doi:10.5194/acp-4-1461-2004

[19] Ellingson, B. A., Theis, D. P., Tishehenkok, O., Zheng, J., and Truhlar, D. G., "Reaction of Hydrogen Atom with Hydrogen Peroxide," *Journal of Physical Chemistry A*, Vol. 111, No. 51, 2007, pp. 13,554–13,566.
doi:10.1021/jp077379x

[20] Baulch, D. L., Bowman, C. T., Cobos, C. J., Cox, R. A., Just, T., Kerr, J. A., Pilling, M. J., Stocker, D., Troe, J., Tsang, W., Walker, R. W., and Warnatz, J., "Evaluated Kinetic Data for Combustion Modeling: Supplement II," *Journal of Physical and Chemical Reference Data*, Vol. 34, No. 3, 2005, pp. 757–1397.
doi:10.1063/1.1748524

[21] Michael, J. V., Su, M. C., Sutherland, J. W., Carroll, J. J., and Wagner, A. F., "Rate Constants for $H + O_2 + M = HO_2 + M$ in Seven Bath Gases," *Journal of Physical Chemistry A*, Vol. 106, No. 21, 2002, pp. 5297–5313.
doi:10.1021/jp020229w

[22] Fernandes, R. X., Luther, K., Troe, J., and Ushakov, V. G., "Experimental and Modeling Study of the Recombination Reaction $H + O_2(+M) \rightarrow HO_2(+M)$ Between 300 and 900 K, 1.5 and 950 bar, and in the Bath Gases M = He, Ar, and N_2," *Physical Chemistry Chemical Physics*, Vol. 10, No. 29, 2008, pp. 4313–4321.
doi:10.1039/b804553d

[23] Cohen, N., and Westberg, K. R., "Chemical Kinetic Data Sheets for High-Temperature Chemical Reactions," *Journal of Physical and Chemical Reference Data*, Vol. 12, No. 3, 1983, pp. 531–590.
doi:10.1063/1.555692

[24] Naudet, V., Javoy, S., and Paillard, C. E., "A High Temperature Chemical Kinetics Study of the Reaction: $OH + Ar = H + O + Ar$ by Atomic Resonance Absorption Spectrophotometry," *Combustion Science and Technology*, Vol. 164, No. 1, 2001, pp. 113–128.
doi:10.1080/00102200108952164

[25] Tsang, W., and Hampson, R. F., "Chemical Kinetic Data Base for Combustion Chemistry. Part I. Methane and Related Compounds," *Journal of Physical and Chemical Reference Data*, Vol. 15, No. 3, 1986, pp. 1087–1253.
doi:10.1063/1.555759

[26] Kappel, Ch., Luther, K., and Troe, J., "Shock Wave Study of the Unimolecular Dissociation of H_2O_2 in its Falloff Range and of its Secondary Reactions," *Physical Chemistry Chemical Physics*, Vol. 4, No. 18, 2002, pp. 4392–4398.
doi:10.1039/b204364e

[27] Kitano, S., Fukao, M., Susa, A., Tshboi, N., Hayashi, A. K., and Koshi, M., "Spinning Detonation and Velocity Deficit in Small Diameter Tubes," *Proceedings of the Combustion Institute*, Vol. 32, No. 2, 2009, pp. 2355–2362.
doi:10.1016/j.proci.2008.06.119

[28] Mozurkewich, M., and Benson, S. W., "Self-Reaction of HO_2 and DO_2: Negative Temperature Dependence and Pressure Effects," *International Journal of Chemical Kinetics*, Vol. 17, No. 8, 1985, pp. 787–807.
doi:10.1002/kin.550170802

[29] Kircher, C. C., and Sander, S. P., "Kinetics and Mechanism of HO_2 and DO_2 Disproportionations," *Journal of Physical Chemistry A*, Vol. 88, 1984, pp. 2082–2091.
doi:10.1021/j150654a029

[30] Kanno, N., Tonokura, K., Tezaki, A., and Koshi, M., "Water Dependence of the HO_2 Self Reaction: Kinetics of the HO_2-HO_2 Complex," *Journal of Physical Chemistry A*, Vol. 109, No. 14, 2005, pp. 3153–3158.
doi:10.1021/jp044592+

[31] Sellevag, S. R., Georgievshii, Y., and Miller, J. A., "The Temperature and Pressure Dependence of the Reactions $H + O_2(+M) \rightarrow HO_2(+M)$ and $H + OH(+M) \rightarrow H_2O(+M)$," *Journal of Physical Chemistry A*, Vol. 112, No. 23, 2008, pp. 5085–5095.
doi:10.1021/jp711800z

[32] Mertens, J. D., Kalitan, D. M., Barrett, A. B., and Petersen, E. L., "Determination of the Rate of $H + O_2 + M = HO_2 + M$ (M = N_2, Ar, H_2O) from Ignition of Syngas at Practical Conditions," *Proceedings of the Combustion Institute*, Vol. 32, No. 1, 2009, pp. 295–303.
doi:10.1016/j.proci.2008.06.163

[33] Troe, J., "Detailed Modeling of the Temperature and Pressure Dependence of the Reaction $H + O_2(+M) \rightarrow HO_2(+M)$," *Proceedings of the Combustion Institute*, Vol. 28, No. 2, 2000, pp. 1463–1469.
doi:10.1016/S0082-0784(00)80542-1

[34] Nielsen, O. J., Sillesen, A., Luther, K., and Troe, J., "Hydrogen Atom Yields in the Pulse Radiolysis of Hydrogen. Reactions with Oxygen, Nitrosyl Chloride, and Hydrogen Iodide," *Journal of Physical Chemistry*, Vol. 86, No. 15, 1982, pp. 2929–2935.
doi:10.1021/j100212a025

[35] Baldwin, R. R., "Comment to 'Rates of Some Atomic Reactions Involving Hydrogen and Oxygen'," *Proceedings of the Combustion Institute*, Vol. 9, 1963, pp. 218–219.

[36] Kochubei, V. F., and Moin, F. B., "Kinetics of Reactions of Atomic Hydrogen with Oxygen," *Ukrainian Chemical Journal*, Vol. 39, No. 9, 1973, pp. 888–892.

[37] Wong, W., and Davis, D. D., "A Flash Photolysis-Resonance Fluorescence Study of the Reaction of Atomic Hydrogen with Molecular Oxygen $H + O_2 + M \rightarrow HO_2 + M$," *International Journal of Chemical Kinetics*, Vol. 6, No. 3, 1974, pp. 401–416.
doi:10.1002/kin.550060310

[38] Bishop, W. P., and Dorfman, L. M., "Pulse Radiolysis Studies. XVI. Kinetics of the Reaction of Gaseous Hydrogen Atoms with Molecular Oxygen by Fast Lymax-α Absorption Spectrophotometry," *Journal of*

Chemical Physics, Vol. 52, No. 6, 1970, pp. 3210–3216.
doi:10.1063/1.1673460
[39] Ahumada, J. J., Michael, J. V., and Osborne, D. T., "Pressure Dependence and Third Body Effects on the Rate Constants for H + O_2, H + NO, and H + CO," *Journal of Chemical Physics*, Vol. 57, No. 9, 1972, pp. 3736–3745.
doi:10.1063/1.1678839
[40] Ishikawa, Y., Sugawara, K., and Sato, S., "The Rate Constants for H and *D*-Atom Additions to O_2, NO, Acetylene, and 1, 3-Butadiene," *Bulletin of the Chemical Society of Japan*, Vol. 52, No. 12, 1979, pp. 3503–3506.
doi:10.1246/bcsj.52.3503
[41] Hasegawa, K., and Asaba, T., "Shock Tube Study of H_2-O_2 Reaction at Relatively High Pressures and Low Temperatures," *Journal of the Faculty of Engineering, University of Tokyo. Series B*, Vol. 31, 1972, pp. 515–526.
[42] Getzinger, R. W., and Blair, L. S., "Recombination in the Hydrogen-Oxygen Reaction: A Shock Tube Study with Nitrogen and Water Vapour and Third Bodies," *Combustion and Flame*, Vol. 13, No. 3, 1969, pp. 271–284.
doi:10.1016/0010-2180(69)90005-4
[43] Peeters, J., and Mahnen, G., "Reaction Mechanisms and Rate Constants of Elementary Steps in Methane–Oxygen Flames," *Proceedings of the Combustion Institute*, Vol. 14, No. 1, 1973, pp. 133–146.
doi:10.1016/S0082-0784(73)80015-3
[44] Atkinson, R., Baulch, D. L., Cox, F. A., Hampson, R. F., Kerr, J. A., and Troe, J., "Evaluated Kinetic and Photochemical Data for Atmospheric Chemistry: Supplement III," *Journal of Physical and Chemical Reference Data*, Vol. 18, No. 2, 1989, pp. 881–1097.
doi:10.1063/1.555832
[45] Javoy, S., Naudet, V., Abid, S., and Paillard, C. E., "Elementary Reaction Kinetics Studies of Interest in H_2 Supersonic Combustion Chemistry," *Experimental Thermal and Fluid Science*, Vol. 27, No. 4, 2003, pp. 371–377.
doi:10.1016/S0894-1777(02)00241-8
[46] Srinivasan, N. K., and Michael, J. V., "The Thermal Decomposition of Water," *International Journal of Chemical Kinetics*, Vol. 38, No. 3, 2006, pp. 211–219.
doi:10.1002/kin.20172
[47] Troe, J., and Ushakov, V. G., "SACM/CT Study of the Dissociation/Recombination Dynamics of Hydrogen Peroxide on an Ab Initio Potential Energy Surface," *Physical Chemistry Chemical Physics*, Vol. 10, No. 26, 2008, pp. 3915–3924.
doi:10.1039/b803320j
[48] Klemm, R. B., Payne, W. A., and Stief, L. J., "Absolute Rate Parameters for Reaction of Atomic Hydrogen with H2O2," *Proceedings of the 1st Symposium on Chemical Kinetics Data for the Upper and Lower Atmosphere*, Wiley-Interscience, New York, 1975, pp. 61–72.
[49] Michael, J. V., Whytock, D. A., Lee, J. H., Payne, W. A., and Steif, L. J., "Absokute Rate Constant for the Reaction of Atomic Chlorine with Hydrogen Peroxide Vapor over the Temperature Range 265–400 K," *Journal of Chemical Physics*, Vol. 67, No. 8, 1977, pp. 3533–3536.
doi:10.1063/1.435351
[50] Albers, E. A., Hoyermann, K., Wagner, H. G., and Worfrum, J., "Absolute Measurements of Rate Coefficients for the Reactions of H and O Atoms with H_2O_2 and H_2O," *Proceedings of the Combustion Institute*, Vol. 13, No. 1, 1971, pp. 81–88.
doi:10.1016/S0082-0784(71)80012-7
[51] Baldwin, R. R., and Walker, R. W., "Rate Constants for Hydrogen + Oxygen System, and for H Atoms and OH Radicals + Alkenes," *Journal of the Chemical Society Faraday Transactions 1*, Vol. 75, 1979, pp. 140–154.
doi:10.1039/f19797500140
[52] Keyser, L. F., "Absolute Rate Constant and Branching Fractions for H + HO_2 Reaction from 245 to 300 K," *Journal of Physical Chemistry*, Vol. 90, No. 13, 1986, pp. 2994–3003.
doi:10.1021/j100404a040
[53] Sridharan, U. C., Qlu, L. X., and Kaufman, F., "Kinetics and Product Channels of the Reactions of HO_2 and H Atoms at 296 K," *Journal of Physical Chemistry*, Vol. 86, No. 23, 1982, pp. 4569–4574.
doi:10.1021/j100220a023
[54] Baldwin, R. R., Fuller, M. E., Hillman, J. S., Jackson, D., and Walker, R. W., "Second Limit of Hydrogen + Oxygen Mixtures: The Reaction H + HO_2," *JJournal of the Chemical Society Faraday Transactions 1*, Vol. 70, 1974, pp. 635–641.
doi:10.1039/F19747000635
[55] Baldwin, R. R., and Walker, R. W., "Rate Constants for Hydrogen + Oxygen System, and for H Atoms and OH Radical + Alkanes," *Journal of the Chemical Society Faraday Transactions 1*, Vol. 75, 1979, pp. 140–154.
doi:10.1039/f19797500140
[56] Hidaka, Y., Taniguchi, T., Tanaka, H., Kamesawa, T., Inami, K., and Kawano, H., "Shock-Tube Study of CH_2O Pyrolysis and Oxidation," *Combustion and Flame*, Vol. 92, No. 4, 1993, pp. 365–376.
doi:10.1016/0010-2180(93)90149-W
[57] Day, M. J., Thompson, K., and Dixon-Lewis, G., "Some Reactions of Hydroperoxyl and Hydroxyl Radicals at High Temperatures," *Proceedings of the Combustion Institute*, Vol. 14, No. 1, 1972, pp. 47–59.
doi:10.1016/S0082-0784(73)80008-6
[58] Mousavipour, S. H., and Saheb, V., "Theoretical Study on the Kinetic and Mechanism of H + HO_2 Reaction," *Bulletin of the Chemical Society of Japan*, Vol. 80, No. 10, 2007, pp. 1901–1911.
doi:10.1246/bcsj.80.1901
[59] Karkach, S. P., and Osherov, V. I., "Ab Initio Analysis of the Transition States on the Lowest Triplet H_2O_2 Potential Surface," *Journal of Chemical Physics*, Vol. 110, No. 24, 1999, pp. 11918–11927.
doi:10.1063/1.479131
[60] Hippler, H., Neunaber, H., and Troe, J., "Shock wave studies of the reactions $HO + H_2O_2 = H_2O + HO_2$ and $HO + HO_2 = H_2O + O_2$ Between 930 and 1680 K," *Journal of Chemical Physics*, Vol. 103, No. 9, 1995, pp. 3510–3516.
doi:10.1063/1.470235
[61] Keyser, L. F., "Kinetics of the Reaction $OH + HO_2 = H_2O + O_2$ from 254 to 382 K," *Journal of Physical Chemistry*, Vol. 92, No. 5, 1988, pp. 1193–1200.
doi:10.1021/j100316a037
[62] Sivaramakrishnan, R., Comandini, A., Tranter, R. S., Brezinsky, K., Davis, S. G., and Wang, H., "Combustion of CO/H_2 Mixtures at Elevated Pressures," *Proceedings of the Combustion Institute*, Vol. 31, No. 1, 2007, pp. 429–437.
doi:10.1016/j.proci.2006.08.057
[63] Srinivasan, N. K., Su, M. C., Sutherland, J. W., Michael, J. V., and Ruscic, B., "Reflected Shock Tube Studies of High-Temperature Rate Constants for $OH + NO_2 = HO_2 + NO$ and $OH + HO_2 = H_2O + O_2$," *Journal of Physical Chemistry A*, Vol. 110, No. 21, 2006, pp. 6602–6607.
doi:10.1021/jp057461x
[64] Hong, Z., Vasu, S. S., Davidson, D. F., and Hanson, R. K., "Experimental Study of the Rate of $OH + HO_2 = H_2O + O_2$ at High Temperatures Using the Reverse Reaction," *Journal of Physical Chemistry A*, Vol. 114, No. 17, 2010, pp. 5520–5525.
doi:10.1021/jp100739t
[65] Gonzalez, C., Theisen, J., Zhu, L., Schelegel, H. B., Hase, W. L., and Kaise, E. W., "Kinetics of the Reaction Between OH and HO_2 on the Singlet Potential Energy Surface," *Journal of Physical Chemistry A*, Vol. 95, 1991, pp. 6784–6792.
doi:10.1021/j100171a010
[66] Gonzalez, C., Theisen, J., Schlegel, H. B., Hase, W. L., and Kaiser, E. W., "Kinetics of the Reaction Between OH and HO_2 on the Triplet Potential Energy Surface," *Journal of Physical Chemistry A*, Vol. 96, 1992, pp. 1767–1774.
doi:10.1021/j100183a051
[67] Germann, T. C., and Miller, W. H., "Quantum Mechanical Pressure-Dependent Reaction and Recombination Rates for $O + OH = H + O_2$, HO_2," *Journal of Physical Chemistry A*, Vol. 101, 1997, pp. 6358–6357.
doi:10.1021/jp9703622
[68] Kee, R. J., Rupley, F. M., Miller, J. A., Coltrin, M. E., Grcar, J. F., Meeks, E., Moffat, H. K., Lutz, A. E., Dixon-Lewis, G., Smooke, M. D., Warnatz, J., Evans, G. H., Larson, R. S., Mitchell, R. E., Petzold, L. R., Reynolds, W. C., Caracotsions, M., Stewart, W. E., Glaborg, P., Wang, C., McLellen, C. L., Adigun, O., Houf, W. G., Chou, C. P., Miller, S. F., Ho, P., Young, P. D., and Young, D. J., CHEMKIN Release 4.1., Reaction Design, San Diego, CA, 2005.
[69] Petersen, E. L., Davidson, D. F., Röhrig, M., and Hanson, R. K., "High-Pressure Shock-Tube Measurements of Ignition Times in Stoichiometric $H_2/O_2/Ar$ Mixtures," *Proceedings of the 20th International Symposium on Shock Waves*, Pasadena, CA, World Scientific, River Edge, NJ, 23–28 July 1995, pp. 941–946.
[70] Slack, M. W., "Rate Coefficient for $H + O_2 + M = HO_2 + M$ Evaluated from Shock Tube Measurements of Induction Times," *Combustion and Flame*, Vol. 28, 1977, pp. 241–249.
doi:10.1016/0010-2180(77)90031-1
[71] Bhaskaran, K. A., Gupta, M. C., and Just, Th., "Shock Tube Study of the Effect of Unsymmetric Dimethyl Hydrazine on the Ignition Characteristics of Hydrogen–Air Mixtures," *Combustion and Flame*, Vol. 21, No. 1, 1973, pp. 45–48.
doi:10.1016/0010-2180(73)90005-9
[72] Catherina, J. W., Nagumo, Y., and Koshi, M., "Third Body Effect on the

Characteristics of Hydrogen Combustion," *Hydrogen Energy Progress XII*, edited by Z. Q. Mao, and T. N. Veziroglu, International Assoc. for Hydrogen Energy, Beijing, 2000, pp. 610–615.

[73] Dowdy, D. R., Smith, D. B., Taylor, S. C., and Williams, A., "The Use of Expanding Spherical Flames to Determine Burning Velocities and Stretch Effects in Hydrogen/Air Mixtures," *Proceedings of the Combustion Institute*, Vol. 23, No. 1, 1990, pp. 325–332. doi:10.1016/S0082-0784(06)80275-4

[74] Aung, K. T., Hassan, I., and Faeth, G. M., "Flame Stretch Interactions of Laminar Premixed Hydrogen/Air Flames at Normal Temperature and Pressure," *Combustion and Flame*, Vol. 109, Nos. 1–2, 1997, pp. 1–24. doi:10.1016/S0010-2180(96)00151-4

[75] Tse, S. D., Zhu, D. L., and Law, C. K., "Morphology and Burning Rates of Expanding Spherical Flames in H_2/O_2/Inert Mixtures up to 60 Atmospheres," *Proceedings of the Combustion Institute*, Vol. 28, No. 2, 2000, pp. 1793–1800. doi:10.1016/S0082-0784(00)80581-0

[76] Kwon, O. C., and Faeth, G. M., "Flame/Stretch Interactions of Premixed Hydrogen-Fueled Flames: Measurements and Predictions," *Combustion and Flame*, Vol. 124, No. 4, 2001, pp. 590–610. doi:10.1016/S0010-2180(00)00229-7

[77] Troe, J., "The Colourful World of Complex-Forming Bimolecular Reactions," *Journal of the Chemical Society, Faraday Transactions*, Vol. 90, No. 16, 1994, pp. 2303–2317. doi:10.1039/ft9949002303

[78] Skrebkov, O. V., Myagkov, Yu. P., Karkach, S. P., Vasil'ev, V. M., and Smirnov, A. L., "Formation Mechanism of the Excited $OH(^2\Sigma^+)$ Radical During the Ignition of the Diluted H2-O2 Mixture by Shock Waves," *Doklady Physical Chemistry (Translation of the physical chemistry section of Doklady Akademii Nuak)*, Vol. 383, Nos. 4/6, 2002, pp. 93–96. doi:10.1023/A:1015368709347

[79] Skrebkov, O. V., Karkach, S. P., Vasil'ev, V. M., and Smirnov, A. L., "Hydrogen–Oxygen Reactions behind Shock Waves Assisted by $OH(^2\Sigma^+)$ Formation," *Chemical Physics Letters*, Vol. 375, Nos. 3–4, 2003, pp. 413–418. doi:10.1016/S0009-2614(03)00875-3

[80] Skrebkov, O. V., and Karkach, S. P., "Vibrational Nonequilibrium and Electronic Excitation in the Reaction of Hydrogen with Oxygen Behind a Shock Wave," *Kinetics and Catalysis*, Vol. 48, No. 3, 2007, pp. 367–375. doi:10.1134/S0023158407030044

[81] Skrebkov, O. V., Karkach, S. P., Ivanova, A. N., and Kostenko, S. S., "Vibrational Nonequilibrium of the HO_2 Radical in the Reaction Between Hydrogen and Oxygen at $1000 < T < 1200$ K," *Kinetics and Catalysis*, Vol. 50, No. 4, 2009, pp. 461–471. doi:10.1134/S0023158409040016

[82] Sander, S. P., Golden, D. M., Kurylo, M. J., Moortgat, G. K., Keller-Rudek, H., Wine, P. H., Ravishankara, A. R., Kolb, E. E., Molina, M. J., Finlayson-Pitts, B. J., Huie, R. E., and Orkin, V. L., "Chemical Kinetics and Photochemical Data for Use in Atmospheric Studies," NASA JPL Publ. 06-2, 2006.

[83] Dunlea, E. J., and Ravishankara, A. R., "Measurement of the Rate Coefficient for the Reaction of $O(^1D)$ with H_2O and Re-Evaluation of the Atmospheric OH Production Rate," *Physical Chemistry Chemical Physics*, Vol. 6, No. 13, 2004, pp. 3333–3340. doi:10.1039/b402483d

T. Lieuwen
Associate Editor